© 2021 The Authors
946

Water Practice & Technology Vol 16 No 3
doi: 10.2166/wpt.2021.040

First investigations on removal of nitrazepam from water using biochar derived from macroalgae low-cost adsorbent: kinetics, isotherms and thermodynamics studies

Mazen K. Nazal*, Durga Rao and Nabeel Abuzaid

Center for Environment and Water, Research Institute, King Fahad University for Petroleum and Minerals (KFUPM), Dhahran, Saudi Arabia 31261

*Corresponding author. E-mail: mazennazal@kfupm.edu.sa

Abstract

Emerging contaminants such as pharmaceutical compounds offer potential hazards to the aquatic environment and human health. In this paper, the adsorptive removal of the drug Nitrazepam from water was investigated for the first time using biochar prepared from *Sargassum* macroalgae. The removal efficiency of Nitrazepam using 1 g/L of *Sargassum* macroalgae-derived biochar was 98% with a maximum adsorption capacity of 143.12 mg/g. Effects of solution pH, adsorbent mass, adsorbate concentration, contact time and temperature on the removal of Nitrazepam were investigated. Different adsorption isotherms and kinetics were also tested. It was found that the solution pH slightly influenced the removal efficiency. The adsorption data fit the Freundlich isotherm model and the adsorption process of Nitrazepam onto *Sargassum* macroalgae-derived biochar is spontaneous, endothermic and followed the pseudo-second-order kinetics. Based on this work, it was determined that the low-cost *Sargassum* macroalgae-derived biochar adsorbent could be a promising adsorbent to remove Nitrazepam from water effectively.

Key words: adsorption isotherms, adsorption kinetics, pharmaceutical compounds, water treatment

Highlights

- A biochar prepared from macroalgae was investigated for Nitrazepam removal from water.
- The adsorbent has high efficiency and adsorption capacity for Nitrazepam emerging contaminant.
- The kinetics and thermodynamics of Nitrazepam adsorption were studied.
- The adsorption process was spontaneous, endothermic and thermodynamically favorable.
- Mixed mechanism was dominated by physisorption and followed pseudo second-order kinetics.

INTRODUCTION

Pharmaceutical compounds and their metabolites as emerging contaminants in the environment have recently been given more attention. They are considered as potentially serious threats to the environment and human health (Desbiolles *et al.* 2018). Although the concentrations of pharmaceutical compounds and their metabolites are low in the environment, their harmfulness and risk to humans and animals are very high (Boxall *et al.* 2012). Their presence in the environment may create drug resistance amongst pathogens and lead to many negative impacts such as convulsion,

Water Practice & Technology Vol 16 No 3
doi: 10.2166/wpt.2021.040

brain damage, cancer diseases, reproductive behavioral disorder, liver damage, cardiovascular diseases and lung defects as well as disturbances in gene expression and other deleterious ecotoxicological effects on aquatic organisms (Saravanan *et al.* 2014; Peltzer *et al.* 2017). Pharmaceutical compounds are discharged to the environment and water resources through different sources (Ilyas *et al.* 2020). Several studies indicate that a huge number (~10,000) of pharmaceutical compounds are prescribed for human and veterinary treatments (Boxall *et al.* 2012; Caldwell *et al.* 2014) and about ~ 10–90% of the evoked pharmaceutical compounds are excreted in their parent form, whereas others are excreted as metabolites or conjugated forms from the human body (Hirsch *et al.* 1999; Kummerer 2009). The pharmaceutical compounds excreted by patients reach the soil, drinking water, groundwater, lakes, rivers and oceans (Li *et al.* 2013; Schaider *et al.* 2014). Other major sources of pharmaceutical compounds in aquatic environments are the disposal of expired pharmaceutical products, hospital wastewater, manufacturing wastes, and veterinary contaminants (Vieno Tuhkanen & Kronberg 2007; Phillips *et al.* 2010; Vulliet & Cren-Olivé 2011; Tewari *et al.* 2013). Pharmaceutical compounds entering the soil infiltrate the groundwater, and it can reach seawater through agricultural runoff from fields that are treated with livestock slurries contaminated with pharmaceutical compounds (Kummerer 2010). Among the pharmaceutical compounds, psychiatric drugs such as benzodiazepines (e.g. Diazepam, Temazepam and Nitrazepam) are used to treat short-term sleeping problems (insomnia) and sometimes applied to treat epilepsy when other medications fail. They are widely prescribed and frequently detected in different environmental media such as drinking water (Lv *et al.* 2019), wastewaters (Thiebault *et al.* 2017a), surface water (Calisto & Esteves 2009) and sediment (Thiebault *et al.* 2017b) due to their inefficient treatment (Thiebault *et al.* 2017c). Hence, proper removal of these compounds from the aquatic environment is highly essential. The above facts have been considered by many researchers, and many techniques have been applied for removal of pharmaceutical compounds from wastewater such as adsorption (Naghipour *et al.* 2018; Bhowmik *et al.* 2020; Debnath *et al.* 2020; Zahra *et al.* 2020), ion exchange, precipitation, coagulation, chlorination, sedimentation, sand filtration, biological treatment, membrane separation, advanced oxidation and ozonation (Westerhoff *et al.* 2005; Snyder *et al.* 2007; Ikehata *et al.* 2008). Among these techniques, adsorption is one of the most widely used methods for the removal of pharmaceuticals from water. Adsorption technique is simple, effective, well established, adaptable to many treatment formats and relatively inexpensive. Other advantages include the fact the adsorption does not produce sludge and has a capability to remove most forms of organic material (Fakhri & Adami 2014; Khadir *et al.* 2020). The cost of adsorption depends mainly on the type of adsorbent used. This was the driving force to investigate different adsorbents from different sources such as activated carbon, powdered activated carbon, activated alumina, charcoal, brick powder, activated sludge, zeolites and biomass. Each of these materials has advantages and disadvantages. However, biomass is renewable as well as considerably cheaper and more abundant than other commercially available materials. In particular, naturally available macroalgae have many advantages. Their cell wall structure and components contain cellulose, alginate and other polysaccharides. These components have many chemical functional groups such as carboxylic acid, hydroxyls, and amines that provide high affinity and selectivity towards organic compounds such as Nitrazepam. These ecofriendly macroalgae and their derived biochar adsorbents showed promising results in removing inorganic and organic pollutants such as heavy metals (Nazal 2019) and phenolic compounds (Eugenia *et al.* 2006; Nazal *et al.* 2020). However, to the best of our knowledge, there is no information available on the adsorptive removal of Nitrazepam from water. Therefore, in this study, for the first time, the adsorptive performance of biochar derived from *Sargassum* macroalgae for Nitrazepam was investigated. The effects of pH, adsorbent mass, and adsorbate concentration on the adsorption efficiency were studied. The experimental results at equilibrium were fitted with the most frequently adsorption isotherms and kinetics models. The thermodynamics parameters of Nitrazepam adsorption were also calculated.

Water Practice & Technology Vol 16 No 3
doi: 10.2166/wpt.2021.040

EXPERIMENTAL DETAILS

Materials

The hypnotic drug Nitrazepam was purchased from Sigma-Aldrich, USA. All the chemicals (i.e. sodium hydroxide, sodium chloride and nitric acid) were analytical reagent (AR) grade and purchased from Merck, Germany. The Acetonitrile (99.9%) HPLC grade solvent, used as mobile phase, was purchased from Fisher Scientific, Germany. Deionized water was used for the experiment.

Adsorbent preparation

Sargassum macroalgae (SM), collected from the coastal water of the Arabian Gulf close to the Saudi Arabia, was thoroughly washed, and then dried in the oven. A biochar derived from *Sarrgassum* macroalgae (BSM) was prepared through thermal pyrolysis of the dried SM under an inert nitrogen atmosphere without any chemical treatment. The detailed preparation procedure and characterization of adsorbents have been reported elsewhere (Nazal *et al.* 2020). Briefly, the dried SM was thermally treated under nitrogen atmosphere in a furnace at 500 °C for 2 hours. Washed material was dried at 110 °C for 48 hours. The resulting biochar was preserved in a tightly closed container to be used later for the adsorption experiment. The point of zero charge pH, at which the net charge of the adsorbent is neutral, was measured by mixing 50 mg of adsorbent in 20 mL of 0.5 M NaCl solutions having different pH values (2–10) for 24 hours at room temperature. Initial and final pH values were recorded using an OAKTON PC2700 pH meter.

Preparation of adsorbate solution

A standard stock solution of 1000 mg/L of Nitrazepam (NZP) was prepared by dissolving the required amount of NZP in methanol. Subsequent test solutions were prepared from the stock solution by appropriate dilution with deionized water. Figure 1 shows the chemical structure of NZP, and Table 1 presents its main physical and chemical properties.

Figure 1 | Nitrazepam chemical structure.

Table 1 | Physical and chemical properties of Nitrazepam

Property	Description
Molecular formula	$C_{15}H_{11}N_3O_3$
Molecular weight	281.27 g/mol
Melting point	255 °C
Boiling point	506.9 °C
Solubility	29.9 mg/L
pK_{a1} and pK_{a2}	3.2 and 10.8

Water Practice & Technology Vol 16 No 3
doi: 10.2166/wpt.2021.040

Analytical method

Concentrations of NZP before and after the adsorption experiments were analyzed in triplicate and measured using High Performance Liquid Chromatography coupled with a Diode Array Detector (HPLC-DAD) at 273 nm wavelength. The chromatographic conditions are summarized in Table 2.

Table 2 | Chromatographic conditions

Parameter	Description
Instrument	Agilent 1200 Series HPLC
Injection volume	10 μL
Column temperature	25 °C
Column	Waters Symmetry® C18, 250 × 4.6 mm, 5 μm
Flow rate	1 mL/min
Detector	Diode Array Detector (HPLC-DAD)
Mobile phase	A: Acetonitrile 70% B: DI water 30%
Wavelength	273 nm

Effect of the weight of adsorbent

To study the effect of the weight of added adsorbents (SM and BSM), different masses (5–250 mg) of adsorbents were added to 25 mL of NZP (5 mg/L) solutions. The resultant solutions were agitated at 24 °C and 140 rpm for 5 days.

Effect of pH

The effect of pH on the adsorptive removal of NZP using *Sargassum* macroalgae adsorbents before and after pyrolysis was studied in pH ranging from 2 to 10. The pH was adjusted by 1.0 M NaOH and 2% HNO_3. 25 mg of adsorbent were mixed with 25 mL of NZP (5 mg/L) and kept in a water bath shaker (BS-31, Lab Companion, Korea) for 5 days, at 24 °C, at a shaking speed of 140 rpm.

Effect of NZP initial concentration and adsorption isotherms

The effect of NZP concentration, in the range of 1 mg/L to 30 mg/L, on the removal efficiency of SM and BSM adsorbents was studied at a constant temperature of 24 °C. Fixed quantities of adsorbents of 1 g/L and 0.2 g/L of SM and BSM, respectively, were used. The resulting solutions were agitated for 5 days. The adsorption isotherms of NZP onto SM and BSM were investigated by fitting the equilibrium adsorption data with the most frequently used isotherm models (i.e. Freundlich, Langmuir and Temkin). Table 3 shows the linear equations of the used isotherm models.

Table 3 | Mathematical linear equations of the three used isotherm models

Isotherm model	Equation	Plot	Reference
Freundlich	$\ln(q_e) = \ln(K_f) + \frac{1}{n}\ln(C_e)$	$\ln(q_e)$ *vs* $\ln(C_e)$	Freundlich (1906)
Langmuir	$\frac{C_e}{q_e} = \frac{1}{bQ_{max}} + \frac{C_e^n}{Q_{max}}$	$\frac{C_e}{q_e}$ *vs* C_e	Langmuir (1916)
Temkin	$q_e = \frac{RT}{b_T}\ln(A_T) + \frac{RT}{b_T}\ln(C_e)$	q_e *vs* $ln(C_e)$	Temkin & Pyzhev (1940)

Water Practice & Technology Vol 16 No 3
doi: 10.2166/wpt.2021.040

where, q_e (mg/g) is the adsorption capacity, C_e (mg/L) is the NZP concentration at equilibrium. K_f (mg/g)(L/mg)$^{1/n}$ and n (dimensionless) are the Freundlich model parameters. Q_{max} (mg/g) is the maximum monolayer adsorption capacity in the Langmuir model and b is the Langmuir constant. In the Temkin model, A_T (L/g) is the equilibrium binding constant, b_T is the Temkin constant, R (J/K mol) is the ideal gas constant and T (K) is the temperature in Kelvin.

The removal efficiency was calculated using the following equation:

$$Removal\ \% = \frac{(C_o - C_e)}{C_o} 100\% \tag{1}$$

Equation (2) was used to calculate the separation factor (R_L) from the Langmuir constant:

$$R_L = \frac{1}{(1 + b\ C_o)} \tag{2}$$

Effect of contact time and adsorption kinetics

In order to study the effect of contact time on the removal efficiency, fixed weights of 25 mg of SM and BSM adsorbents were added to 25 mL of NZP (5 mg/L) solutions in capped vials. The mixtures were agitated for different time intervals (i.e. 0.5, 1, 2, 4, 6, 8, 24, 72,120 and 144 hours). The solutions were then filtered and analyzed to measure the NZP concentration. The adsorption data were then fitted with different adsorption kinetic models (presented in Table 4).

Table 4 | Mathematical linear equations of the used kinetics and intra-particle diffusion kinetic models

Kinetics model	Equation	Plot	Reference
Pseudo-first order (PFO)	$\ln(q_e - q_t) = \ln(q_e) - k_1 t$	$\ln(q_e - q_e) vs\ t$	Lagergren (1898)
Pseudo-second order (PSO)	$\frac{t}{q_t} = \frac{1}{q_e^2 k_2} + \frac{t}{q_e}$	$\frac{t}{q_t}\ vs\ t$	Ho & McKay (1998)
Elovich	$q_t = \frac{1}{b}\ln(ab) + \frac{1}{b}\ln(t)$	$q_t\ vs\ ln(t)$	Chien & Clayton (1980)
Intra-particle diffusion	$q_t = k_{id} t^{0.5} + C$	$q_t\ vs\ t^{0.5}$	Weber Asce & Morris (1963)

where q_t (mg/g) is the adsorption capacity at a certain time t (min), in pseudo-first order and pseudo-second order kinetics, and k_1 (min^{-1}) and k_2 (g/mg/min) are the rate constants respectively. In the Elovish model, a (mg/g/min) is the initial adsorption rate and b (g/mg) is the desorption constant. k_{id} (mg/g/min$^{0.5}$) and C (mg/g) in the Weber equation are the intra-particle diffusion rate constant and the constant related to the thickness of the boundary layer, respectively.

Effect of temperature

The effect of temperature, in the range of 24–45 °C, on the adsorption of NZP (5 mg/L) onto SM and BSM adsorbents was studied. A fixed adsorbent quantity of 1 g/L was used, and the solutions were agitated at 140 rpm for 5 days. The adsorption free energy (ΔG), enthalpy (ΔH) and entropy (ΔS) were calculated using the following equations:

$$\Delta G^o = \Delta H - T\Delta S \tag{3}$$

$$\mathrm{Ln}\, K_d = \frac{\Delta S^o}{R} - \frac{\Delta H^o}{RT} \tag{4}$$

Water Practice & Technology Vol 16 No 3
doi: 10.2166/wpt.2021.040

where T is the temperature in Kelvin (K), R is the gas constant and equal to 0.008314 kJ/mol K, and K_d is the adsorption distribution coefficient in L/g.

RESULTS AND DISCUSSION

Adsorbents characterization

The detailed characterization was performed, discussed and reported in our previous publication (Nazal *et al.* 2020). Briefly, the surface morphology of SM before and after pyrolysis is shown in Figure 2. It has been found that the surface of SM (shown in Figure 2(a)) is covered with biological species (Diatoms), which may result in covering the active adsorption sites and explains the low adsorption capacity of macroalgae, before pyrolysis, for the NZP compound. After pyrolysis, the surface of BSM (shown in Figure 2(b)) became more clear with some openings and holes, which may explain the improvement in the adsorption performance of BSM as a result of increasing the contact area between NZP and the active adsorption sites on the surface.

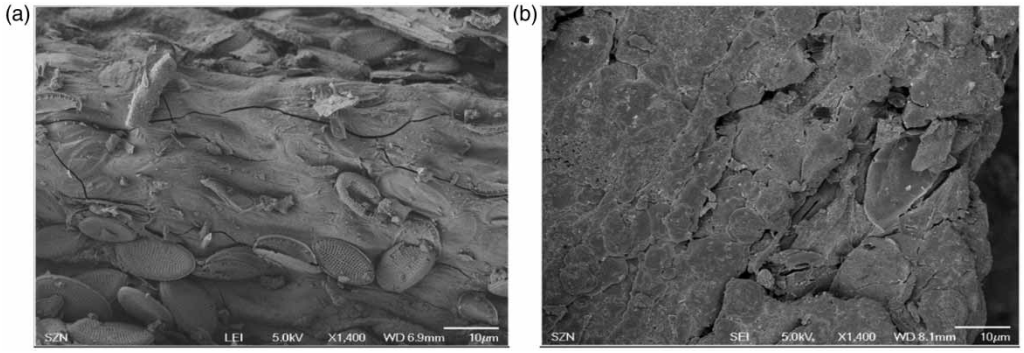

Figure 2 | SEM images of *Sargassum* macroalgae surface (a) before (SM) and (b) after the thermal pyrolysis (BSM).

The proximate analysis results showed that in the SM the percentage of fixed carbon (46.45%) increased after pyrolysis to be 74.57%, which indicates the increase of hydrophobic carbon contents of BSM. On the other hand, the FTIR showed the surface of both SM and BSM has different functional groups (e.g. hydroxyl (OH), carboxylic acid (COOH) and carbonyl (C = O)) that may contribute to the interaction between the used adsorbents and Nitrazepam, the emerging pollutant, through the hydrogen bonding. Moreover, the surface area (3.8 $m^2 g^{-1}$) and pore volume (0.006 mL g^{-1}) of BSM were larger than the surface area (1.34 $m^2 g^{-1}$) and pore volume (0.005 mL g^{-1}) of SM before pyrolysis. These findings may contribute to elaborating the difference between the adsorption capacity of MA and BSM adsorbents as well as explaining the adsorption mechanism onto their surfaces.

Effect of adsorbent weight

Figure 3 shows the effect of the loaded SM and BSM adsorbents' dose on the removal efficiency of NZP. It has been found that the maximum removal efficiencies of 60 and 98% are obtained using 4 g/L and 1 g/L of SM and BSM adsorbents respectively. After the treatment of SM adsorbent, the removal efficiency was significantly improved. This might be attributed to the increase of the BSM adsorbent's surface functional groups, which in turn enhanced the acid-base and electrostatic interactions between the pharmaceutical compound NZP and the BSM adsorbent. Figure 3 also shows that the removal efficiency increases by increasing the adsorbent weight. This is due to the increase of adsorption sites.

Water Practice & Technology Vol 16 No 3
doi: 10.2166/wpt.2021.040

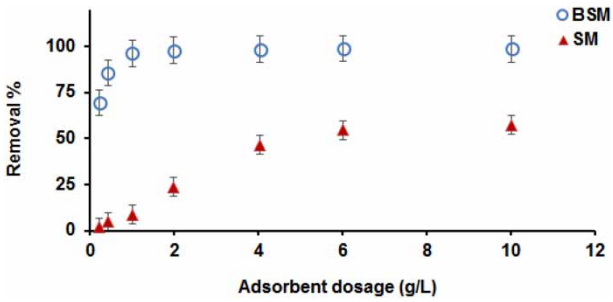

Figure 3 | Effect of SM and BSM adsorbents dose on the removal of NZP (5 mg/L) at 24 °C.

pH effect

The effect of pH on the removal efficiency of NZP onto SM and BSM adsorbents is shown in Figure 4. It has been found that the pH of the solution slightly influences the removal efficiency. This may be attributed to the slight change in the adsorbate-adsorbent electrostatic interaction. Considering the pKa values of NZP (3.2 and 10.8) and the pH_{pzc} of SM (5.06) and BSM (9.87), it is expected that, in the range of pH between 5 and 10, the anionic form of NZP dominates and the surface charges of SM and BSM are negative and positive, respectively. Therefore, at pH 5, the removal efficiency of NZP using SM slightly decreased, while it slightly increased using the BSM adsorbent. Hence, in all the adsorption experiments, the NZP solutions having a pH of 5.8 were used without any adjustment.

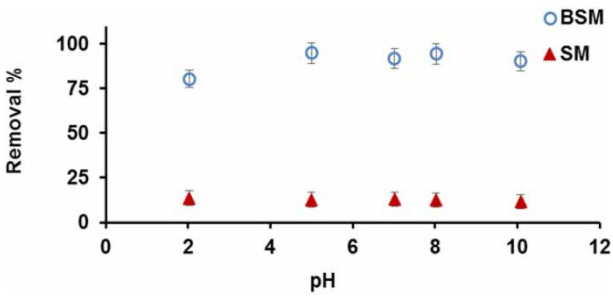

Figure 4 | Effect of pH on the removal efficiency of NZP using SM and BSM adsorbents.

Effect of NZP initial concentrations and the adsorption isotherms

Figure 5(a) shows the effect of NZP concentration on the removal efficiencies of SM and BSM adsorbents. It has been found that using SM (1 g/L) is not efficient for removing the NZP compound under the experimental conditions. In the case of using BSM (0.2 g/L), the maximum removal efficiency for NZP was 75%, which is 20 times higher than the maximum removal efficiency of an SM adsorbent. However, their removal efficiencies decreased as the initial concentration of NZP increased. This is attributed to the saturation of the adsorbents' surface and the increase of repulsion between the adsorbed molecules on the surface and free molecules in solution. Because of the low adsorption capacity of SM, the adsorption experimental data of SM could not be fitted with the isotherm models. However, different isotherm models were tested for NZP adsorption onto BSM adsorbents. The plots of the linear forms of the tested adsorption isotherm models are presented in Figure 5(b)–5(d).

Water Practice & Technology Vol 16 No 3
doi: 10.2166/wpt.2021.040

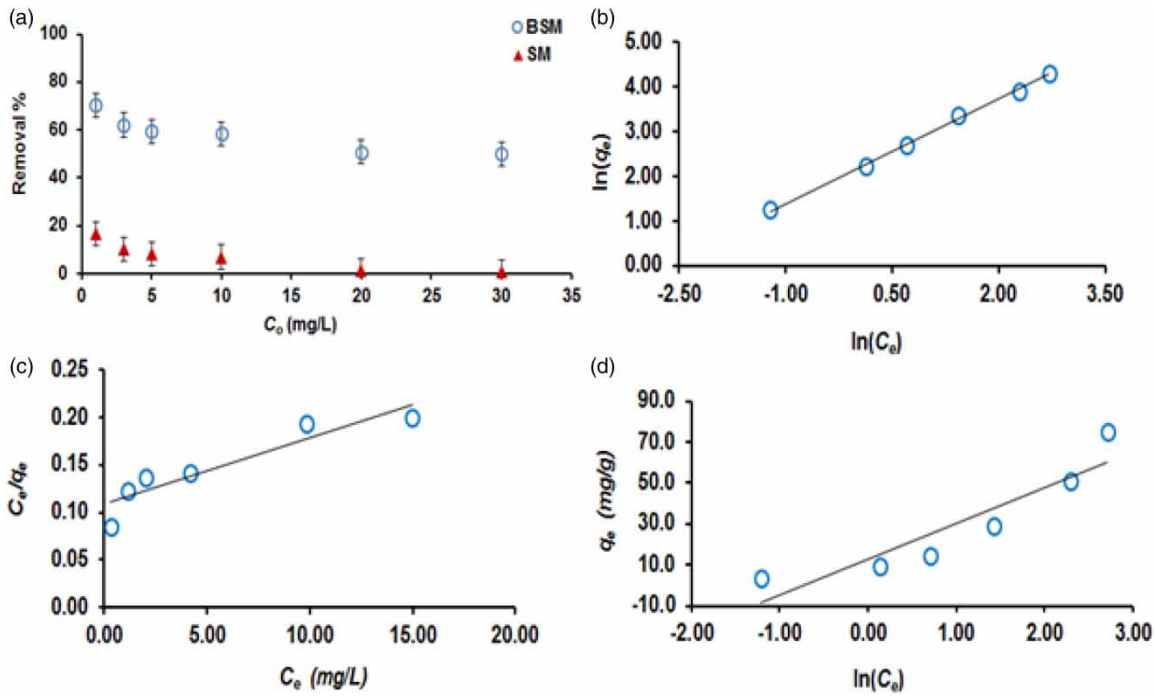

Figure 5 | (a) effect of NZP concentration on the removal efficiencies of SM and BSM adsorbents at a 24 °C, linear least squares fit of (b) Freundlich model, (c) Langmuir model and (d) Temkin model.

The summation of relative error (SER) between $q_{e\ exp.}$ and $q_{e\ pred}$. was calculated using Equation (5) and used to validate fitting the adsorption results with the isotherm models.

$$SRE = \sum_{i=0}^{n}\left[\frac{(q_{e\ exp.} - q_{e\ pred})_i^2}{q_{e\ exp}}\right] \tag{5}$$

The models' parameters for NZP adsorption onto BSM are summarized in Table 5. These parameters were calculated from the slope and the intercept of the linear form of the corresponding adsorption isotherm model. It has been found that the Freundlich isotherm is the best fit to the experimental adsorption results with a squared correlation coefficient (R^2) of 0.9980 and summation of relative error (SRE) of 0.3448. This reveals that the BSM adsorbent's surface is heterogeneous and the physical adsorption mechanism is predominant. The n and K_f values higher than 1 indicate that the adsorption of NZP onto BSM is favorable. The higher magnitude of these values corresponds to greater heterogeneity and higher adsorption capacity respectively (Li Quinlivan & Knappe 2002).

Table 5 | Freundlich, Langmuir and Temkin's parameters for NZP adsorption onto BSM adsorbent

Freundlich			
n	K_f ((mg/g)(L/mg)$^{1/n}$)	R^2	SER
1.28	8.83	0.9980	0.3448
Langmuir			
b ((L/mg))	Q_o (mg/g)	R^2	SER
0.0641	143.12	0.8565	1.1672
Temkin			
A_T (L/g)	b_T (kJ/mol)	R^2	SER
1.10	0.1380	0.8482	166.1794

Water Practice & Technology Vol 16 No 3
doi: 10.2166/wpt.2021.040

The value of R_L (0.34), between zero and one, shows the favorability of NZP adsorption. The maximum monolayer adsorption capacity of BSM for NZP is 143.12 mg/g. The interactions between NZP and the BSM surface involve three possible mechanisms. These are (i) electrostatic interaction, (ii) π-π and n-π interactions between the π and n electrons on NZP and π-electrons on the surface of the BSM adsorbent and (iii) hydrogen-bonding interaction.

Effect of contact time and adsorption kinetics

Contact time is a vital parameter affecting the removal efficiency and giving an insight into adsorption kinetics. As shown in Figure 6, the SM and BSM removal efficiencies for NZP increased rapidly in the first 24 hours, which is attributed to the maximum availability of unoccupied adsorption sites on the surface of the adsorbents. Then, they reached equilibrium within 48 and 120 hours using SM and BSM adsorbents, respectively. It is also apparent that the removal efficiency of BSM is higher than SM. This is due to the dominance of ionic forms of NZP molecules as well as the negative and positive charge of the SM and BSM surfaces, respectively, at the pH (5.8) of the solutions.

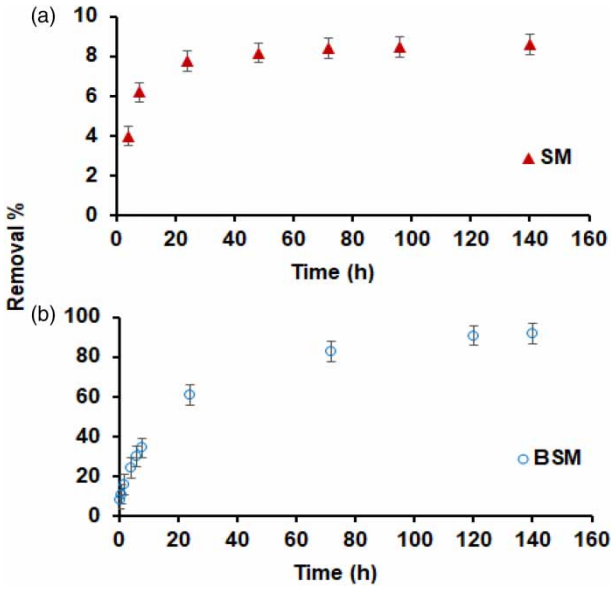

Figure 6 | Contact time effect on the removal efficiency of (a) SM and (b) BSM for NZP. Concentration of NZP is 5 mg/L, adsorbent dosage concentration is 1 g/L and shaking speed is 140 rpm at a temperature of 24 °C.

Figure 7 shows the plots of the linearized kinetics models (i.e. PFO, PSO and Elovich). The adsorption kinetics' parameters are calculated from the slopes and the intercepts of the corresponding linear plots and summarized in Table 6.

The obtained squared correlation coefficients (R^2) are close to 1 and the q_e experimental ($q_{e\ exp.}$) and q_e predicted ($q_{e\ pred.}$) values are very close to each other in PSO for both adsorbents. Although the R^2 values obtained in the PFO are high, the $q_{e\ exp.}$ and $q_{e\ pred}$ values are not close to each other. In addition, the summation of relative error (SER) between $q_{e\,exp.}$ and $q_{e\,pred}$ was calculated for the tested kinetics models. It has been found that the lowest SER is for PSO. This clearly indicates that the adsorption of NZP on SM and BSM follows the PSO kinetics. This also indicates the involvement of chemisorption in the rate-determining step in the adsorption mechanism (Ho & McKay 1999).

For further investigation of the adsorption mechanism and to know if NZP adsorption onto SM and BSM are described as a diffusion-controlled process, the equilibrium adsorption data were fitted to

Water Practice & Technology Vol 16 No 3
doi: 10.2166/wpt.2021.040

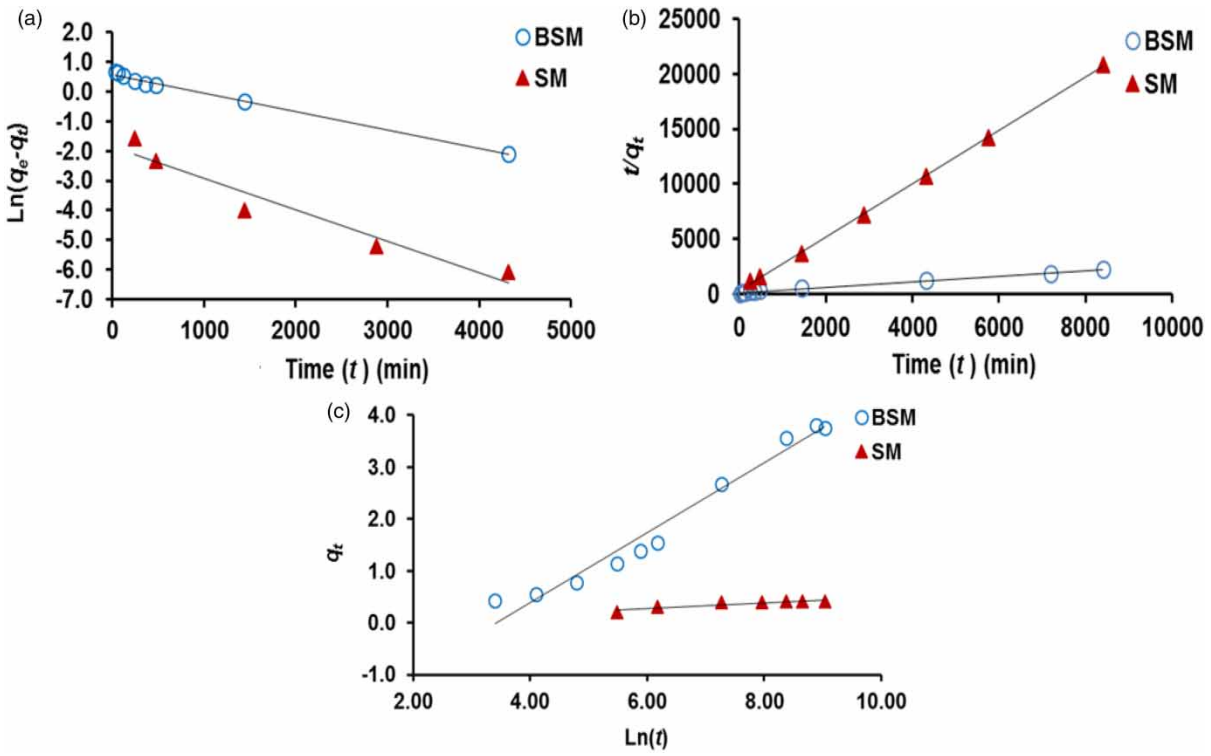

Figure 7 | Linear least square fit for linearized (a) PFO, (b) PSO and Elovich models for NZP adsorption onto SM and BSM adsorbents.

Table 6 | PFO, PSO and Elovich adsorption kinetics parameters for NZP adsorption onto SM and BSM adsorbents

	PFO					
Adsorbent	$q_{e\ exp.}$	$q_{e\ pred.}$	k_1 (1/min)		**SRE**	R^2
BSM	3.81	3.15	0.0006		4.2812	0.9919
SM	0.41	0.21	0.0011		1.1114	0.9398
	PSO					
	$q_{e\ exp.}$	$q_{e\ pred.}$	k_2 (g /mg min)		**SRE**	R^2
BSM	3.81	4.03	0.0004		0.2820	0.9974
SM	0.41	0.41	0.0156		0.0142	0.9996
	Elovich kinetics					
	$q_{e\ exp.}$	$q_{e\ pred.}$	***a*** **(mg/g min)**	***b*** **(g/mg)**	**SRE**	R^2
BSM	3.81	3.77	0.0220	1.49	0.6797	0.9682
SM	0.41	0.44	0.0232	18.76	0.0226	0.8214

Weber and Morris' intra-particle diffusion kinetics model. As shown in Figure 8, plotting q_t versus $t^{0.5}$ reveals two linear parts. This indicates that NZP adsorption onto both adsorbents is governed by two steps of diffusion. The first step is fast and related to the diffusion of NZP from the bulk solution to the available adsorption sites on the surface of the adsorbent, while the second step arises from the adsorption of these compounds to the adsorption sites, and this step occurs more slowly than the first one (Khadir *et al.* 2020). Table 7 summarizes the calculated intra-particle parameters. As shown, k_{id} values of the first step for adsorption of NZP onto SM and BSM adsorbents are higher than k_{id} values of the second step, while the values of the C constant for the first steps are lower than those

Water Practice & Technology Vol 16 No 3
doi: 10.2166/wpt.2021.040

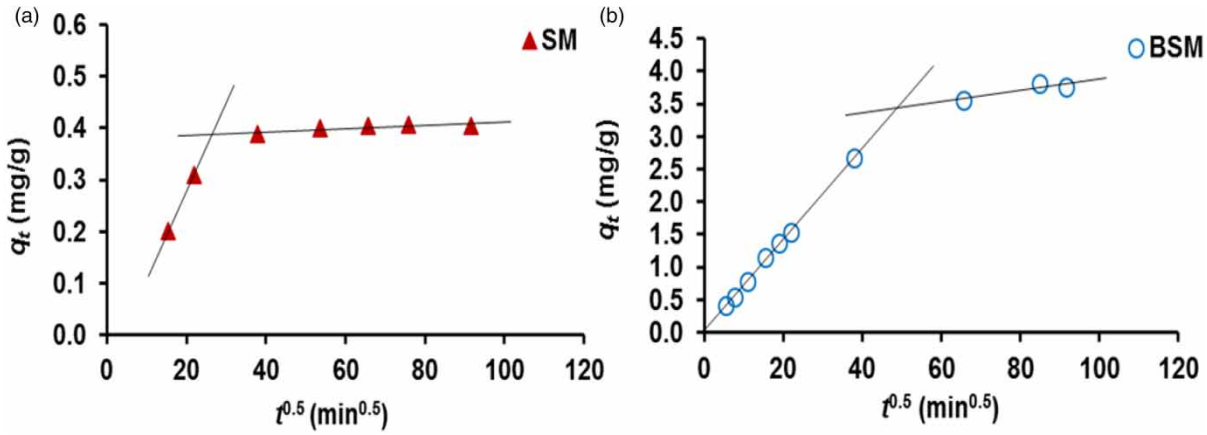

Figure 8 | Intra-particle diffusion plots for NZP adsorption on (a) SM and (b) BSM adsorbents at 24 °C.

Table 7 | Intra-particle calculated parameters for NZP adsorption on SM and BSM adsorbents

	SM		BSM	
Parameter	**1st step**	**2nd step**	**1st step**	**2nd step**
k_{id}	0.0171	0.0001	0.0699	0.0086
C	0.0006	0.397	0.0278	3.0129

in the second steps. This suggests that the thickness of the boundary layer of SM is smaller than that of the boundary layer of BSM. As a result, the adsorption of NZP is faster onto an SM adsorbent.

Thermodynamics of NZP adsorption

The adsorption's enthalpy and entropy were obtained from the slope and intercept of log K_d vs $1/T$ plot (shown in Figure 9). Table 8 summarizes the thermodynamics parameters for NZP adsorption onto SM and BSM adsorbents. It has been found that the free energy (ΔG) values of NZP adsorption onto SM are positive in the studied temperature range (24–45 °C). This indicates that the adsorption is non-spontaneous and thermodynamically unfavorable. However, these values are negative for NZP adsorption onto BSM adsorbents, which confirms that the adsorption is spontaneous and thermodynamically favorable. Decreasing ΔG values with increasing temperature, and positive values of ΔH for NZP adsorption onto SM and BSM adsorbents, indicate that the adsorption process is endothermic. In addition, the low values of ΔG (ranging between −10.73 and − 0.28 kJ/mol) and the obtained value

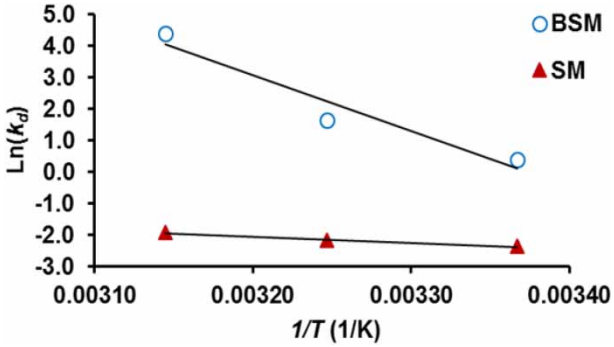

Figure 9 | Plot of ln K_d vs. $1/T$ for NZP adsorption on SM and BSM adsorbents.

Water Practice & Technology Vol 16 No 3
doi: 10.2166/wpt.2021.040

Table 8 | Thermodynamic parameters for the adsorption of NZP on SM and BSM adsorbents

	SM			BSM		
Temperature (K)	ΔG (kJ/mol)	ΔH (kJ/mol)	ΔS (kJ/mol K)	ΔG (kJ/mol)	ΔH (kJ/mol)	ΔS (kJ/mol K)
297	5.89	16.55	0.04	− 0.28	147.51	0.50
308	5.49			− 5.75		
318	5.14			− 10.73		

of ΔH (147.51 kJ/mol) reveals that the adsorption mechanism is mixed and the physical adsorption is predominant (Saha & Chowdhury 2011; Zaghouane-Boudiaf & Boutahala 2011). The small positive entropy values in the adsorption system in this study indicate that randomness increases at the adsorbate/adsorbent interface.

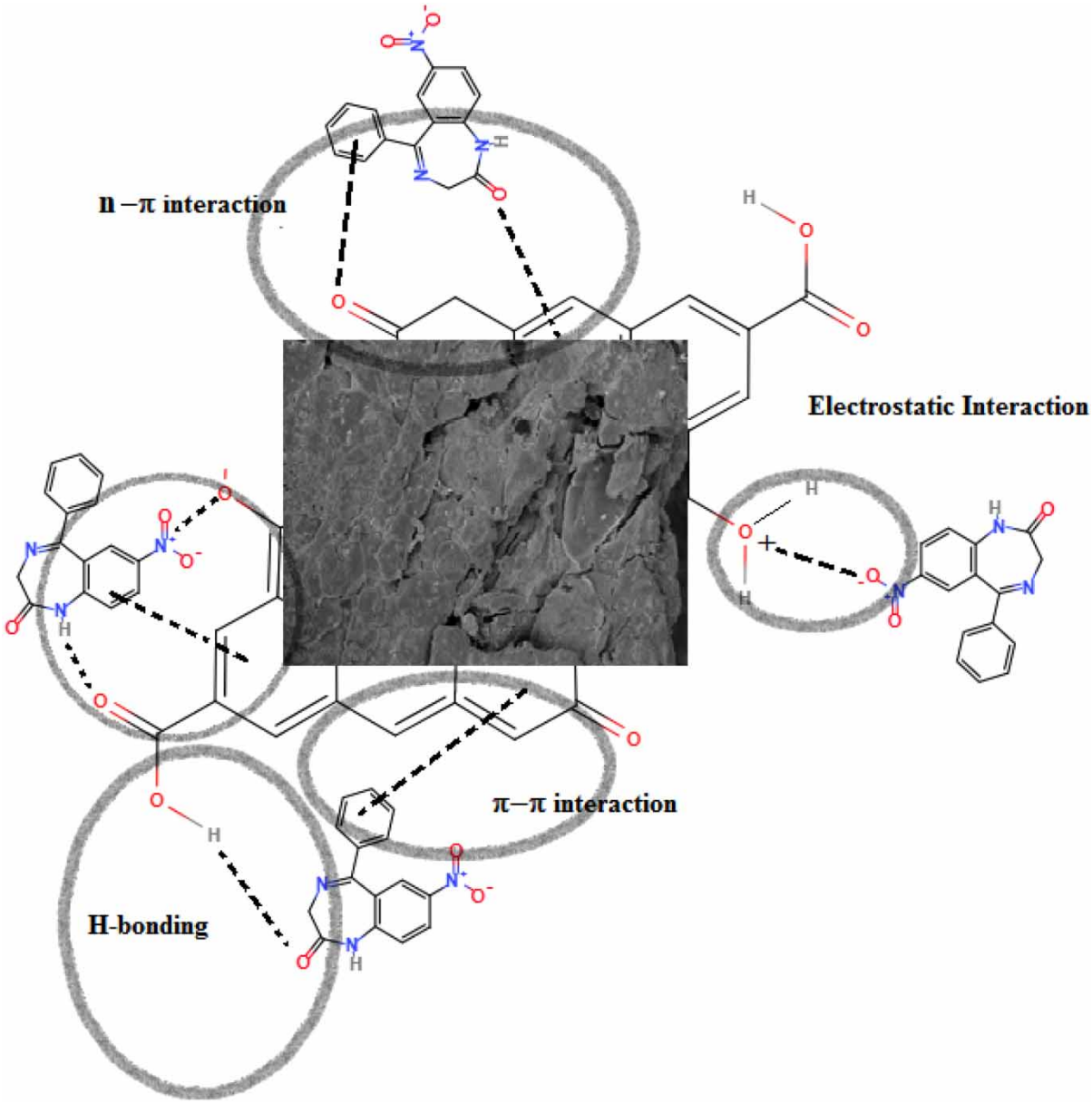

Figure 10 | Schematic illustration of the potential adsorption interactions between Nitrazepam and the biochar derived from *Sargassum* macroalgae.

Water Practice & Technology Vol 16 No 3
doi: 10.2166/wpt.2021.040

Proposed adsorption mechanism of NZP

Generally, the adsorption process of organic compounds onto carbon based material depends on three main factors, namely the nature of the adsorbent and adsorbate (e.g. porosity, size of molecules, functional groups and net charge) and adsorption conditions (e.g. pH and temperature of solution) (Gupta *et al.* 2013). Considering the previously reported characterization results of the SM and BSM adsorbents, NZP molecules may interact with the surface of SM through hydrogen-bonding and electrostatic interactions, while it may interact with the prepared biochar through hydrophobic, π-π and n-π, electrostatic and hydrogen-bonding interactions. Figure 10 illustrates the key adsorption mechanism of NZP onto the surface of the biochar derived from *Sargassum* macroalgae. The proposed mechanism is supported by the obtained adsorption isotherms and thermodynamics results, where the adsorption of Nitrazepam onto both adsorbents is dominated by a physisorption mechanism.

CONCLUSION

For the first time, the adsorptive removal of the pharmaceutical active compound Nitrazepam (NZP) from water was investigated, and the nature and kinetics of its adsorption onto the *Sargassum* macroalgae (SM) and the biochar derived from this macroalgae (BSM) were studied in this work. The removal capability of the macroalgae adsorbent (MA) for the NZP compound was improved after thermal pyrolysis, with a removal efficiency up to 98% and an adsorption capacity of 143 mg/g. The adsorption equilibrium results showed that the adsorption was obtained through a mixed mechanism dominated by physisorption and followed by pseudo-second-order kinetics. The thermodynamics results revealed that the adsorption of NZP onto SM was non-spontaneous and thermodynamically unfavorable, with a positive value of ΔG. However, the adsorption of NZP onto BSM was spontaneous and thermodynamically favorable with a negative value of ΔG. In addition, the adsorption process of NZP onto both adsorbents was endothermic with a positive ΔH. Furthermore, the low values of ΔG and the obtained values of ΔH disclose that the adsorption mechanism is mixed and physical adsorption is predominant. The positive value of ΔS reflected the affinity of the adsorbent toward NZP, indicating an increase in randomness at the liquid/solid interface. The findings in this study showed that the biochar derived from *Sargassum* macroalgae (BSM) could provide a promising adsorbent for removing pharmaceutical compounds from contaminated water.

CONFLICT OF INTEREST

The authors declare that there is no conflict of interest regarding the publication of this article.

DATA AVAILABILITY STATEMENT

All relevant data are included in the paper or its Supplementary Information.

REFERENCES

Bhowmik, M., Debnath, A. & Saha, B. 2020 Effective remediation of an antibacterial drug from aqua matrix using $CaFe_2O_4$/ZrO_2 nanocomposite derived via inorganic chemical pathway: statistical modelling by response surface methodology. *Arabian Journal for Science and Engineering* **45**, 7289–7303. https://doi.org/10.1007/s13369-020-04465-y.

Water Practice & Technology Vol 16 No 3
doi: 10.2166/wpt.2021.040

Boxall, A. B. A., Rudd, M. A., Brooks, B. W., Caldwell, D. J., Choi, K. & Hickmann, S. 2012 Pharmaceuticals and personal care products in the environment: what are the big questions? *Environmental Health Perspectives* **120**, 1221–1229. https://doi.org/10.1016/ j.envint. 2013.06.012.

Caldwell, D. J., Mastrocco, F., Margiotta-Casaluci, L. & Brooks, B. W. 2014 An integrated approach for prioritizing pharmaceuticals found in the environment for risk assessment, monitoring and advanced research. *Chemosphere* **115**, 4–12. https://doi.org/ 10.1016/ j. chemosphere.2014.01.021.

Calisto, V. & Esteves, V. I. 2009 Psychiatric pharmaceuticals in the environment. *Chemosphere* **77**, 1257–1274. doi:10.1016/j.chemosphere.2009.09.021.

Chien, S. H. & Clayton, W. R. 1980 Application of Elovich equation to the kinetics of phosphate release and sorption on soils. *Soil Science Society of America Journal* **44**, 265–268. https://doi.org/10.2136/sssaj1980.03615995004400020013x.

Debnath, B., Majumdar, M., Bhowmik, M., Bhowmik, K. L., Debnath, A. & Roy, D. N. 2020 The effective adsorption of tetracycline onto zirconia nanoparticles synthesized by novel microbial green technology. *Journal of Environmental Management* **261**, 110235.

Desbiolles, F., Malleret, L., Tiliacos, C., Wong-Wah-Chung, P. & Laffont-Schwob, I. 2018 Occurrence and ecotoxicological assessment of pharmaceuticals: is there a risk for the Mediterranean aquatic environment. *Science of the Total Environment* **639**, 1334–1348. https://doi.org/10.1016/j. scitotenv. 2018.04.351.

Eugenia, R., Pilar, R., Roberto, H. & Manuel, E. S. 2006 Biosorption of phenolic compounds by the brown alga *Sargassum muticum*. *Chemical Technology & Biotechnology* **81**(7), 1093–1099. https://doi.org/10.1002/jctb.1430.

Fakhri, A. & Adami, S. 2014 Adsorption and thermodynamic study of Cephalosporins antibiotics from aqueous solution onto MgO nanoparticles. *Journal of the Taiwan Institute of Chemical Engineers* **45**, 1001–1006. https://doi.org/10.1016/j.jtice.2013.09.028.

Freundlich, H. 1906 Over the adsorption in solution. *Journal of Physical Chemistry* **57**, 385–471.

Gupta, V., Kumar R, K., Nayak, A., Saleh, T. A. & Barakat, M. A. 2013 Adsorptive removal of dyes from aqueous solution onto carbon nanotubes: a review. *Advances in Colloid and Interface Science* **193–194**, 24–34.

Hirsch, R., Ternes, T., Haberer, K. & Kratz, K. 1999 Occurrence of antibiotics in the aquatic environment. *Science of the Total Environment* **225**, 109–118. https://DOI.org/10.1016/s0048-9697(98)00337-4.

Ho, Y. & McKay, G. 1998 A comparison of chemisorption kinetic models applied to pollutant removal on various sorbents. *Process Safety and Environmental Protection* **76**, 332–340. https://doi.org/10.1205/095758298529696.

Ho, Y. & McKay, G. 1999 Pseudo-second order model for sorption processes. *Process Biochemistry* **34**(5), 451–465. https://doi.org/10.1016/S0032-9592(98)00112-5.

Ikehata, K., El-Din, M. G. & Snyder, S. A. 2008 Ozonation and advanced oxidation treatment of emerging organic pollutants in water and wastewater. *Ozone: Science & Engineering* **30**, 21–26. https://doi.org/10.1080/01919510701728970.

Ilyas, H., Masih, I. & van Hullebusch, E. D. 2020 Pharmaceuticals' removal by constructed wetlands: a critical evaluation and meta-analysis on performance, risk reduction, and role of physicochemical properties on removal mechanisms. *Journal of Water & Health* **18**(3), 253–291. https://doi.org/10.2166/wh.2020.213.

Khadir, A., Mollahosseini, A., Tehrani, R. M. A. & Negarestani, M. 2020 A review on pharmaceutical removal from aquatic media by adsorption: understanding the influential parameters and novel adsorbents. In: *Sustainable Green Chemical Processes and Their Allied Applications. Nanotechnology in the Life Sciences* (Inamuddin, A. Asiri, eds). Springer, Cham, pp. 207–265. https://doi.org/10.1007/978-3-030-42284-4_8.

Kummerer, K. 2009 The presence of pharmaceuticals in the environment due to human use-present knowledge and future challenges. *Journal of Environmental Management* **90**, 2354–2366. https://doi.org/10.1016/j.jenvman.2009.01.023.

Kummerer, K. 2010 Pharmaceuticals in the environment. *Annual Review of Environment and Resources* **35**, 57–75. https://doi.org/10.1146/annurev-environ-052809-161223.

Lagergren, S. 1898 About the theory of so-called adsorption of soluble substances. *Kungliga Svenska Vetenskapsakademiens Handlingar* **24**, 1–39.

Langmuir, I. 1916 The constitution and fundamental properties of solids and liquids. *Journal of the American Chemical Society* **38**(11), 2221–2295. https://doi.org/10.1021/ja02242a004.

Li, L., Quinlivan, P. A. & Knappe, D. R. 2002 Effects of activated carbon surface chemistry and pore structure on the adsorption of organic contaminants from aqueous solution. *Carbon* **40**(12), 2085–2100. https://doi.org/10.1016/S0008-6223(02)00069-6.

Li, W., Shi, Y., Gao, L., Liu, J. & Cai, Y. 2013 Occurrence and removal of antibiotics in a municipal wastewater reclamation plant in Beijing, China. *Chemosphere* **92**, 435–444. https://doi.org/10.1016/j.chemosphere.2013.01.040.

Lv, J., Zhang, L., Chen, Y., Ye, B., Han, J. & Jin, N. 2019 Occurrence and distribution of pharmaceuticals in raw, finished, and drinking water from seven large river basins in China. *Journal of Water & Health* **17**(3), 477–489. https://doi.org/10.2166/wh.2019.250.

Naghipour, D., Hoseinzadeh, L., Taghavi, K. & Jaafari, J. 2018 Characterization, kinetic, thermodynamic and isotherm data for diclofenac removal from aqueous solution by activated carbon derived from pine tree. *Data in Brief* **18**, 1082–1087. doi: 10.1016/j.dib.2018.03.068.

Nazal, M. K. 2019 'Marine Algae Bioadsorbents for Adsorptive Removal of Heavy Metals'. Advanced Sorption Process Applications, Serpil Edebali, IntechOpen, https://doi.org/10.5772/intechopen.80850.

Water Practice & Technology Vol 16 No 3
doi: 10.2166/wpt.2021.040

Nazal, M. K., Rao, D. & Abuzaid, N. 2020 The nature and kinetics of 2,4-dimethylphenol adsorption in aqueous solution on biochar derived from *Sargassum boveanum* macroalgae. *Journal of Water Supply: Research and Technology-Aqua* **69**(5), 438–452. https://doi.org/10.2166/aqua.2020.142.

Peltzer, P. M., Lajmanovich, R. C., Attademo, A. M., Junges, C. M., Teglia, C. M., Martinuzzi, C., Curi, L., Culzoni, M. J. & Goicoechea, H. C. 2017 Ecotoxicity of veterinary enrofloxacin and ciprofloxacin antibiotics on anuran amphibian larvae. *Environmental Toxicology and Pharmacology* **51**, 114–123. https://doi.org/10.1016/j.etap.2017.01.021.

Phillips, P. J., Smith, S. G., Kolpin, D. W., Zaugg, S. D., Buxton, H. T., Furlong, E. T., Esposito, K. & Stinson, B. 2010 Pharmaceutical formulation facilities as sources of opioids and other pharmaceuticals to wastewater treatment plant effluents. *Environmental Science & Technology* **44**, 4910–4916. https://doi.org/10.1021/es100356f.

Saha, P. & Chowdhury, S. 2011 'Insight into adsorption thermodynamics. Thermodynamics.' Prof. Mizutani Tadashi (Ed.), ISBN: 978-953-307-544-0, InTech, Available from: https://doi.org/10.5772/13474.

Saravanan, M., Hur, J. H., Arul, N. & Ramesh, M. 2014 Toxicological effects of clofibric acidand diclofenac on plasma thyroid hormones of an Indian major carp, *Cirrhinus mrigala* during short and long-term exposures. *Environmental Toxicology and Pharmacology* **38**, 948–958. https://doi.org/ 10. 1016/ j.etap.2014.10.013.

Schaider, L. A., Rudel, R. A., Ackerman, J. M., Dunagan, S. C. & Brody, J. G. 2014 Pharmaceuticals perfluorosurfactants, and other organic wastewater compounds in public drinking water wells in a shallow sand and gravel aquifer. *Science of the Total Environment* **468**, 384–393. https://doi.org/10.1016/j.scitotenv.2013.08.067.

Snyder, S. A., Adham, S., Redding, A. M., Cannon, F. S., DeCarolis, J., Oppenheimer, J., Wert, E. C. & Yoon, Y. 2007 Role of membranes and activated carbon in the removal of endocrine disruptors and pharmaceuticals. *Desalination* **202**, 156–181. https://doi.org/10.1016/j.desal.2005.12.052.

Temkin, M. & Pyzhev, V. 1940 Kinetics of ammonia synthesis on promoted iron catalysts. *Acta Physiochim URSS* **12**(3), 217–222.

Tewari, S., Jindal, R., Kho, Y. L., Eo, S. & Choi, K. 2013 Major pharmaceutical residues in wastewater treatment plants and receiving waters in Bangkok, Thailand, and associated ecological risks. *Chemosphere* **91**(5), 697–704. https://doi.org/10.1016/j.chemosphere.2012.12.042.

Thiebault, T., Fougère, L., Destandau, E., Réty, M. & Jacob, J. 2017a Temporal dynamics of human-excreted pollutants in wastewater treatment plant influents: toward a better knowledge of mass load fluctuations. *Science of the Total Environment* **596–597**, 246–255. https://doi.org/10.1016/j.scitotenv.2017.04.130.

Thiebault, T., Chassiot, L., Fougère, L., Destandau, E., Simonneau, A., Van Beek, P., Souhaut, M. & Chapron, E. 2017b Record of pharmaceutical products in river sediments: a powerful tool to assess the environmental impact of urban management. *Anthropocene* **18**, 47–56. https://doi.org/10.1016/j.ancene.2017.05.006.

Thiebault, T., Boussafir, M. & Le Milbeau, C. 2017c Occurrence and removal efficiency of pharmaceuticals in an urban wastewater treatment plant: mass balance, fate and consumption assessment. *Journal of Environmental Chemical Engineering* **5**, 2894–2902. https://doi.org/10.1016/j.jece.2017.05.039.

Vieno, N., Tuhkanen, T. & Kronberg, L. 2007 Elimination of pharmaceuticals in sewage treatment plants in Finland. *Water Research* **41**, 1001–1012. https://doi.org/10.1016/j.watres.2006.12.017.

Vulliet, E. & Cren-Olivé, C. 2011 Screening of pharmaceuticals and hormones at the regional scale, in surface and groundwaters intended to human consumption. *Environmental Pollution* **159**, 2929–2934. https://doi.org/10.1016/j.envpol.2011.04.033.

Weber, W., Asce Jr., J. M. & Morris, J. C. 1963 Kinetic of adsorption on carbon from solutions. *Journal of the Sanitary Engineering Division* **89**(2), 31–60.

Westerhoff, P., Yoon, Y., Snyder, S. & Wert, E. 2005 Fate of endocrine-disruptor, pharmaceutical, and personal care product chemicals during simulated drinking water treatment processes. **39**(17), 6649–6663. https://doi.org/10.1021/es0484799

Zaghouane-Boudiaf, H. & Boutahala, M. 2011 Adsorption of 2, 4, 5-trichlorophenol by organo-montmorillonites from aqueous solutions: kinetics and equilibrium studies. *Chemical Engineering Journal* **170**, 120–126. https://doi.org/10.1016/j.cej.2011.03.039.

Zahra, S., Reza, F., Leila, V. & Iraj, N. 2020 Adsorptive removal of apramycin antibiotic from aqueous solutions using Tween 80-and Triton X-100 modified clinoptilolite: experimental and fixed-bed modeling investigations. *International Journal of Environmental Health Research* **30**(5), 558–583. https://doi.org/10.1080/09603123.2019.1612039.

First received 9 March 2021; accepted in revised form 20 April 2021. Available online 4 May 2021